Optical and electronic properties of $NiFe_2O_4$ and $CoFe_2O_4$ thin films

R.C. Rai · S. Wilser · M. Guminiak · B. Cai · M.L. Nakarmi

Abstract We report the optical and electronic properties of the inverse spinel ferrite $NiFe_2O_4$ and $CoFe_2O_4$ thin films deposited on single crystal sapphire by electron beam deposition. We carried out variable temperature (78–500 K) transmittance measurements on the thin films to investigate the optical properties and electronic structures of these ferrites. The absorption spectra of both $NiFe_2O_4$ and $CoFe_2O_4$ thin films show insulating characters with Ni (Co) d to d on-site transitions below 3 eV. The energy bands above 3 eV are mainly due to the O 2p to Fe 3d charge transfer transitions. The observed electronic transitions have been assigned based on the first principles calculations and comparisons with structurally similar Ni and Co-containing compounds. The Co^{2+} d to d transition in the $CoFe_2O_4$ thin film shows a strong temperature dependence, likely due to the spin-charge coupling effect.

1 Introduction

Spinel ferrites, such as $NiFe_2O_4$ and $CoFe_2O_4$, have attracted a great deal of interest because of their potential applications in the upper microwave and lower millimeter wave ranges, spin filters, and heterostructures devices [1–4]. In particular, $NiFe_2O_4$ (NFO) and $CoFe_2O_4$ (CFO) have

R.C. Rai (✉) · S. Wilser · M. Guminiak
Department of Physics, SUNY College at Buffalo, Buffalo, NY 14222, USA
e-mail: rairc@buffalostate.edu
Fax: +1-716-8784421

B. Cai · M.L. Nakarmi
Department of Physics, Brooklyn College of the CUNY, Brooklyn, NY 11210, USA

been used to fabricate superlattice structures and multiferroic heterostructures that demonstrate magnetoelectric coupling between ferromagnetic and ferroelectric thin film layers [5–9]. The thin films of these inverse ferrites display relatively weaker physical properties compare to the bulk counterparts [10–12]. The coupling of spin, charge, and lattice degrees-of-freedom in these ferrites is expected to be significant due to the exchange interactions between the two different types of magnetic ions residing on different crystallographic sites [2, 13]. Consequently, the physical properties of these ferrites could be strongly influenced by such coupling processes. Understanding the optical properties, electronic structures, and coupling effects of these ferrites is essential not only to improve thin film quality but also to develop potential applications.

Inverse spinel ferrites have a chemical formula AB_2O_4 (where A = Ni, Co, and B = Fe) in which A^{2+} [Ni^{2+} ($3d^8$) and Co^{2+} ($3d^7$)] ions reside on octahedral sites and Fe^{3+} ($3d^5$) ions reside equally among tetrahedral (A-sites) and octahedral sites (B sites). Oxygen ions are found in fcc close-packed structures. The unit cell contains 32 O-atoms in a cubic lattice with 8 T_d (FeO_4) and 16 O_h (AO_6 and FeO_6) occupied sites. Both NFO and CFO are in high-spin states with the electronic configurations of $t_{2g}^6 e_g^2$ and $t_{2g}^5 e_g^2$, respectively. Similarly, NFO and CFO are ferrimagnetic insulators with high Curie temperatures $T_C = 850$ and 790 K, respectively [3, 8]. Optics is a local probe that can provide insight into the local crystal structures, such as tetrahedral and octahedral environments, and the corresponding electronic structures of inverse spinel ferrites. In particular, electronic absorption spectroscopy is useful in the investigation of the electronic transitions arising due to different local structures, and the analysis of these transitions using ligand field theory can reveal valuable information about the electronic structures of this family.

In this paper, we present the optical properties and electronic structures of NFO and CFO thin films deposited on (0001) sapphire substrate by the electron beam deposition technique. We used the optical spectroscopy to investigate the electronic transitions of the spinel ferrite thin films. The observed electronic transitions have been assigned based on the first principles calculations and comparisons with the electronic transitions in the structurally similar Ni and Co-containing compounds. The absorption spectra of NFO and CFO thin films show insulating characters with metal d to d on-site transitions below ~3 eV and O 2p to Fe 3d charge transfer transitions above 3 eV. No intervalence and interlattice charge transfer excitations [14–16] have been observed in our samples, and we argue that these transitions would have very small oscillator strengths compared to the observed metal d to d on-site and the O 2p to Fe 3d charge transfer transitions. In addition, an electronic transition (Co^{2+} d to d transition at ~1.75 eV) in the CFO film displays a discontinuous change at ~200 K, likely due to the spin-charge coupling effect.

2 Methods

We used a reactive electron beam deposition system to prepare the thin films of inverse spinel ferrites on (0001) sapphire and (100) $SrTiO_3$ substrates. The target pellets were prepared from high purity (99.9%) powder samples by cold pressing with a hydraulic press and subsequently sintering them at 1000°C for 12 hours in a tube furnace. During the evaporation process, the chamber base pressure was ~10^{-7} Torr and an oxygen partial pressure was maintained at ~4×10^{-4} Torr, and substrates were kept at room temperature. Our thin film thickness ranges from 50 to 200 nm. All thin films were post-deposition annealed in the mixture of O_2 and air for 3 hours at temperatures ranging from 400 to 600°C to improve the stoichiometry and crystal quality. Although we prepared thin films on both sapphire and $SrTiO_3$ substrates, we have only presented the data collected from the thin films grown on sapphire substrates. In fact, the thin films deposited on both substrates show identical optical properties up to ~3.1 eV. Note that $SrTiO_3$ substrates have strong absorption above ~3.1 eV, while sapphire substrates are transparent well above 6.0 eV and offer a wider optical window for the studies.

The crystal structures and surface morphologies of thin films were studied by a Philips X$\overset{\grave{}}{P}$ert-MPD X-ray diffractometer (XRD) and a digital instrument atomic force microscope (AFM), respectively. We used a dual-beam UV-VIS-NIR spectrophotometer (Shimadzu UV 3101PC) and a continuous flow helium cryostat to measure variable-temperature (78–500 K) transmittance in the wavelength range of 200–3000 nm (0.41–6.2 eV), with a spectral resolution of 1 nm. We also measured the reflectance of thin
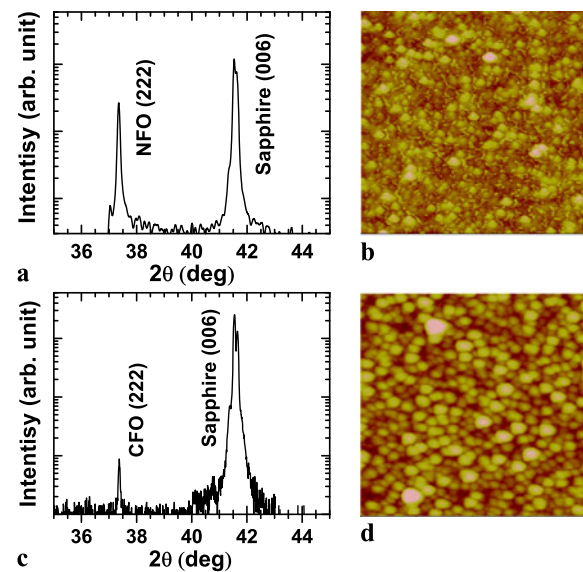

Fig. 1 X-ray diffraction patterns and (1 μm × 1 μm) AFM images of (**a**), (**b**) a 120 nm NFO thin film and (**c**), (**d**) a 100 nm CFO thin film grown on (0001) sapphires and post-deposition annealed at 500°C

films at room temperature. The absorption (α) was extracted from the transmittance data by using the equation, $\alpha = -\ln(T)/d$, where T is the transmittance and d is the film thickness. For room temperature data, we also used equation $\alpha = -\ln[T/(1-R)]/d$, where R is the reflectance, in order to check the contribution of the reflectance in the absorption spectra. Both the equations gave very similar absorption spectra mainly due to the fact that the reflectance of NFO and CFO thin films were very small, and we only present the absorption spectra extracted using the first equation with just transmittance.

3 Results and discussion

Figure 1(b) and (d) show the AFM images of 120 nm NFO and 100 nm CFO thin films grown on (0001) sapphire substrates, respectively. The AFM images show smooth surfaces (with surface roughness < 5 nm) for both the samples. Figure 1(a) and (c) show the X-ray diffraction patterns of the NFO and CFO thin films, respectively. The diffraction patterns show the (222) plane as the preferred crystalline orientation for both the NFO and CFO thin films. Although we scanned the XRD in the 10–80 deg range, we have presented the data between 35 and 45 deg for clarity. The assignment of XRD peaks are based on the NFO and CFO powder XRD data. These XRD data clearly show that the thin films have a good quality with a preferred plane. It is likely that these films have polycrystalline form because the films were grown on sapphire at room temperature. The proper post-deposition annealing of thin films in a mixture of oxygen and air is the key to improve the film quality. It
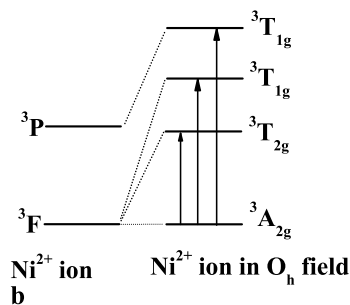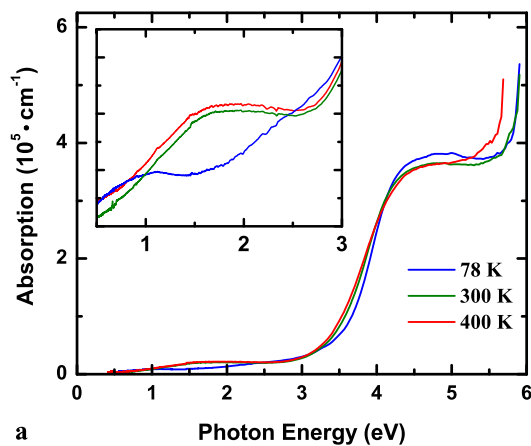
Fig. 2 (**a**) Electronic absorption spectra of a 120 nm NFO thin film at 78, 300, and 400 K, respectively. The *inset* shows the close-up view of the low energy absorption spectra. (**b**) A schematic energy level diagram for the Ni^{2+} (3d^8) ion in an octahedral field and three spin-allowed Ni^{2+} d to d electronic transitions in NiO$_6$
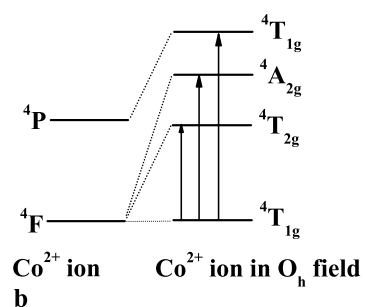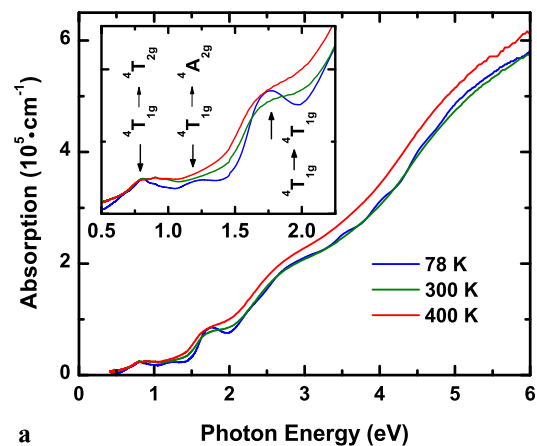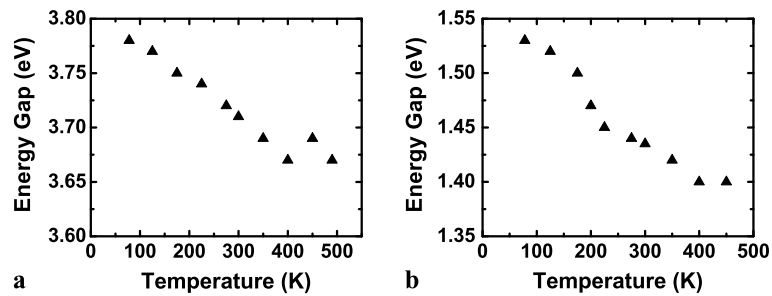

Fig. 3 (**a**) Electronic absorption spectra of a 100 nm CFO thin film at 78, 300, and 400 K, respectively. The *inset* shows the close-up view of the low energy absorption spectra. (**b**) A schematic energy level diagram for the Co^{2+} (3d^7) ion in an octahedral field and three spin-allowed Co^{2+} d to d electronic transitions in CoO$_6$

is noted that sapphire was chosen as substrate in our studies for two reasons, although it is not the best for epitaxial grow of these ferrites from the structure point of view. First, sapphire offers a much wider window for optical studies, as compared to MgO and SrTiO$_3$ substrates that are structurally similar to these ferrites. Second, the optical probe is a microscopic probe that can be used to study the local structures of the sample regardless of its polycrystalline or single crystal nature.

Figure 2(a) shows the electronic absorption spectra of the NFO film on (0001) sapphire at the representative temperatures. The spectra show a weak excitation centered at ∼1.5 eV and a strong excitation peak at ∼4.5 eV. Transmittance spectra (not shown here) of NFO films display high transparency (<75%) for photon energy up to 3 eV. The inset in Fig. 2(a) highlights the ∼1.50 eV band, which red shifts and becomes even weaker below 175 K. Figure 2(b) shows the schematic energy level diagram for the Ni^{2+} (3d^8) ion in an octahedral field and the possible electronic transitions within the Ni d states [17]. In an octahedral crystal field, the degeneracy of Ni^{2+} (3d^8) states is lifted, allowing 3 possible on-site Ni d to d transitions, $^3A_{2g}$(F) → $^3T_{2g}$(F), $^3A_{2g}$(F) → $^3T_{1g}$(F), and $^3A_{2g}$(F) → $^3T_{1g}$(P). These three spin-allowed transitions have weak oscillator strengths and

they overlapped each other, resulting in a single broad band. The temperature dependence of this feature suggests that the local environment of NiO$_6$ changes with cooling. Moreover, weak oscillator strength of the feature is consistent with the fact that these Ni d to d transitions are parity forbidden. The broad and structureless absorption band centered at ∼4.50 eV with a strong oscillator strength is attributed to the O 2p to Fe 3d charge transfer excitations.

Figure 3(a) displays the absorption spectra of the CFO thin film at 78, 300, and 400 K, respectively. The spectra show a typical insulating character with three distinct low energy peaks centered at ∼0.75, 1.25, and 1.75 eV, respectively (inset). These peaks are attributed to spin-allowed Co^{2+} d to d on-site transitions, $^4T_{1g}$(F) → $^4T_{2g}$(F), $^4T_{1g}$(F) → $^4A_{2g}$(F), and $^4T_{1g}$(F) → $^4T_{1g}$(P), respectively, as depicted in the energy level splitting of the Co^{2+} (3d^7) ion in an octahedral field (Fig. 3b) [17]. The electronic excitations above ∼3.00 eV are attributed to the O 2p to Fe 3d charge transfer excitations. Our assignments of electronic transitions are consistent with the theoretical calculations and the reported electronic transitions in the structurally similar Ni and Co-containing compounds [13, 19–22]. The resistivity values, as measured with a four-point probe method, confirm the insulating nature of the thin films. The room temperature

Fig. 4 The energy gap as a
function of temperature of (**a**) a
120 nm NFO thin film (**b**) a 100
nm CFO thin film

resistivity of a 120 nm NFO film is 1.13×10^4 Ω cm and that
of a 100 nm CFO film is 2.66×10^4 Ω cm, respectively.

The comparison of the absorption spectra of the CFO and
NFO films displays similarity in their electronic transitions.
As discussed above, in both ferrites, the low energy transi-
tions below 3 eV are mainly due to the spin-allowed metal d
to d transitions. The spectra (Fig. 2 and Fig. 3) show that
the electronic transitions in CFO have stronger oscillator
strengths than those in NFO, suggesting that the local struc-
ture is significantly distorted for CoO_6 than it is for NiO_6.
We interpret this local distortion to be intrinsic effect, pos-
sibly due to a spin-charge-lattice coupling. Such a distor-
tion of the local structure breaks the crystal field symmetry
of an O_h field and the d to d transitions become allowed
[18]. On the other hand, the $Fe^{3+}(d^5)$ ions in both FeO_6 and
FeO_4 local structures are in high-spin states. As a result, the
Fe^{3+} d to d transitions are not only spin-forbidden, but they
are also parity-forbidden. Therefore, the oscillator strengths
of any Fe^{3+} d to d transitions would be negligibly small and
likely will not appear in the absorption spectra.

Figure 4(a) shows the energy gap of the NFO thin film
as a function of temperature. The energy gap was estimated
from the $(\alpha \cdot E)^2$ versus E (photon energy) graph at each
temperature. For NFO, the direct energy gap E_g is 3.78 eV
at 78 K, which confirms that NFO is a wide band gap insu-
lator. The band gap shows a typical linear dependence with
temperature. We could not draw any decisive conclusion on
a small change observed at around 450 K because of the
limited data points. Based on our data, the NFO thin film
has the O 2p to Fe 3d charge-transfer type energy gap, as
opposed to the theoretically predicted Ni d to d energy gap
of ~1.0 eV [13]. On the other hand, the energy band gap [the
leading edge of $^4T_{1g}(F) \rightarrow {}^4T_{1g}(P)$ transition] of the CFO
film displays a discontinuous change at ~200 K (Fig. 4(b)),
indicating the modifications of the local octahedral crystal
field environment (CoO_6) upon cooling, likely due to the
strong spin-charge coupling effect. Furthermore, the discon-
tinuity of the energy gap is the evidence for the fact that the
electronic excitations within the transition metal d manifold
of CFO are sensitive to the local crystal field environments.
The lattice mismatch between the substrate and CFO might
have contributed to the crystal field distortion in the CFO

films. The strain effects have been reported to play a signif-
icant role on the electronic and magnetic properties of the
spinel ferrites films [12, 23, 24]. The systematic studies of
CFO films deposited on different single crystal substrates
will offer more insight into the role of the lattice mismatch
between the substrate and material, and its overall effect on
the optical properties and electronic structures. The lattice
mismatch and other parameters will be investigated more
thoroughly in future research.

Understanding the electronic structures of these ferrite
thin films is very important to improve thin film quality as
well as to enhance the physical properties, particularly the
magnetic properties for potential applications. In the pre-
vious magnetooptical studies on NFO and CFO [14–16],
the electronic transitions between 0.5 and 5.0 eV were con-
troversially assigned to the inter-valence charge transfer
(IVCT) and inter-sublattice charge transfer (ISCT) transi-
tions. The electronic transitions between two metal ions,
such as between Co^{2+} and Fe^{3+} ions, and between Ni^{2+}
and Fe^{3+} ions are referred to as the IVCT transitions, and
the electronic transitions between Fe^{3+} ions on different
crystallographic sites are referred to as the ISCT transi-
tions [14–16]. These transitions were speculated to be me-
diated by oxygen. Since the electronic wave functions be-
tween two different metal ions do not directly overlap each
other, the transition probability of such IVCT and ISCT
transitions would be either extremely small or negligible.
Therefore, the IVCT and ISCT transitions between differ-
ent metal ions in two sublattices are highly unlikely in the
inverse spinel ferrites. Further, the theoretical calculations
of CFO and NFO do not support the possibility of observ-
ing the electronic transitions between these metal ions be-
low 3 eV, because the (occupied and unoccupied) density of
states of Ni and Fe (Co and Fe) are well separated (>5 eV)
from each other [13]. Indeed, the Ni and Co d to d on-
site transitions are commonly observed in the absorption
spectra of many complex oxides even though they are spin-
allowed but parity-forbidden by the symmetry rules. We ar-
gue that the local structural distortions of MO_6 due to the
coupling effects, asymmetric lattice vibrations that break
the symmetry (i.e., from a centrosymmetric MO_6 to a non-
centrosymmetric MO_6), and the hybridization between the

metal d and oxygen p-states relax the selection rules, allowing the metal d to d on-site transitions. As observed in our spectra, weak oscillator strengths of metal d to d transitions are the characteristics of parity-forbidden but spin-allowed transitions. The magnetic and magneto-dielectric properties will be investigated to elucidate the spin-charge coupling effect in inverse spinel ferrites thin films.

4 Conclusion

We prepared the NFO and CFO thin films on single crystal substrates with very good optical quality. The XRD and AFM studies confirmed that the NFO and CFO thin films have the (222) plane with smooth surfaces (with surface roughness < 5 nm). The absorption spectra of NFO and CFO thin films show insulating characters with the metal d to d on-site transitions below 3 eV and the O 2p to Fe 3d charge transfer transitions above 3 eV. The optical spectra display weak oscillator strengths for the electronic transitions below ∼3 eV, characteristics of the spin-allowed but parity-forbidden metal d to d on-site electronic transitions. We argue that the previously assigned IVCT and ISCT transitions between two metal ions in these ferrites would have very small oscillator strengths compared to the observed metal d to d on-site and the O 2p to Fe 3d charge transfer transitions. Therefore, the IVCT and ISCT transitions in the absorption spectra are ruled out in inverse spinel ferrites. Further, the observed discontinuous change of the ∼1.75 eV electronic transition at ∼200 K in the CFO film is likely due to the spin-charge coupling effect.

References

1. U. Lüders, A. Barthèlémy, M. Bibes, K. Bouzehouane, S. Fusil, E. Jacquet, J.-P. Contour, J.-F. Bobo, J. Fontcuberta, A. Fert, Adv. Mater. **18**, 1733 (2006)
2. Y. Suzuki, Annu. Rev. Mater. Res. **31**, 265 (2001)
3. U. Lüders, M. Bibes, K. Bouzehouane, E. Jacquet, J.-P. Contour, S. Fusil, J.-F. Bobo, J. Fontcuberta, A. Barthèlémy, A. Fert, Appl. Phys. Lett. **88**, 082505 (2006)
4. V. Sepelak, K. Baabe, K. Mienert, K. Schultze, F. Krumeich, F.J. Litterst, K.D. Becker, J. Magn. Magn. Mater. **257**, 377 (2003)
5. S.P. Crane, C. Bihler, M.S. Brandt, S.T.B. Goennenwein, M. Gajek, R. Ramesh, J. Magn. Magn. Mater. **321**, L5 (2009)
6. H. Zheng, J. Wang, S.E. Lofland, Z. Ma, L. Mohaddes-Ardabili, T. Zhao, L. Salamanca-Riba, S.R. Shinde, S.B. Ogale, F. Bai, D. Viehland, Y. Jia, D.G. Schlom, M. Wuttig, A. Roytburd, R. Ramesh, Science **303**, 661 (2004)
7. R.V. Chopdekar, Y. Suzuki, Appl. Phys. Lett. **89**, 182506 (2006)
8. A.V. Ramos, T.S. Santos, G.X. Miao, M.-J. Guittet, J.-B. Moussy, J.S. Moodera, Phys. Rev. B **78**, 180402(R) (2008)
9. U. Lüders, M. Bibes, J.-F. Bobo, M. Cantoni, R. Bertacco, J. Fontcuberta, Phys. Rev. B **71**, 134419 (2005)
10. G. Hu, J.H. Choi, C.B. Eom, V.G. Harris, Y. Suzuki, Phys. Rev. B **62**, R779 (2000)
11. P.C. Dorsey, P. Lubitz, D.B. Chrisey, J.S. Horwitz, J. Appl. Phys. **79**, 6338 (1996)
12. S. Venzke, R.B. van Dover, J.M. Phillips, E.M. Gyorgy, T. Siegrist, C.-H. Chen, D. Werder, R.M. Fleming, R.J. Felder, E. Coleman, R. Opila, J. Mater. Res. **11**, 1187 (1996)
13. Z. Szotek, W.M. Temmerman, D. Ködderitzsch, A. Svane, L. Petit, H. Winter, Phys. Rev. B **74**, 174431 (2006)
14. W.F.J. Fontijn, P.J. van der Zaag, L.F. Feiner, R. Metselaar, M.A.C. Devillers, J. Appl. Phys. **85**, 5100 (1999)
15. B. Zhou, Y. Zhang, Y. Yu, C. Liao, C. Yan, Phys. Rev. B **68**, 024426 (2003)
16. K.J. Kim, H.S. Lee, M.H. Lee, S.H. Lee, J. Appl. Phys. **91**, 9974 (2002)
17. Y. Tanabe, S. Sugano, J. Phys. Soc. Jpn. **9**, 753 (1954)
18. F.A. Cotton, *Chemical Applications of Group Theory* (Wiley, New York, 1990)
19. G.A. Sawatzky, J.W. Allen, Phys. Rev. Lett. **53**, 2339 (1984)
20. J. Schnack, M. Brüger, M. Luban, P. Kögerler, E. Morosan, R. Fuchs, R. Modler, H. Nojiri, R.C. Rai, J. Cao, J.L. Musfeldt, Phys. Rev. B **73**, 094401 (2006)
21. R.C. Rai, J. Cao, L.I. Vergara, S. Brown, J.L. Musfeldt, D.J. Singh, G. Lawes, N. Rogado, R.J. Cava, X. Wei, Phys. Rev. B **76**, 174414 (2007)
22. M.T. Czyzyk, R. Potze, G.A. Sawatzky, Phys. Rev. B **46**, 3729 (1992)
23. A. Lisfi, L.T. Nguyen, J.C. Lodder, C.M. Williams, H. Corcoran, P. Chang, A. Johnson, W. Morgan, J. Magn. Magn. Mater. **290**, 219 (2005)
24. A. Lisfi, C.M. Williams, A. Johnson, L.T. Nguyen, J.C. Lodder, H. Corcoran, P. Chang, W. Morgan, J. Phys., Condens. Matter **17**, 1399 (2005)